only within the four cells of the quiescent center, whereas expression in the *nww* mutant expanded to include a larger number of cells (Fig. 3, I and J).

Because *WOX5* has been shown to be downstream of auxin signaling, we also analyzed pDR5-GFP expression to determine whether auxin signaling is altered in the *nww* mutant root (Fig. 3, K and L, and fig. S7). In WT roots, pDR5-GFP was observed in only the quiescent center and columella cells. In the rescued roots of the *nww* mutant, pDR5-GFP was misexpressed throughout the presumptive root cap. Although auxin signaling still occurs in the *nww* mutant, the altered pDR5-GFP expression pattern suggests that the roots are unable to respond to auxin in an appropriate manner. Thus, the *NWW* genes are required for appropriate development of the quiescent center and the distal root meristem.

Misexpression of *NTT* might be sufficient to transform other stem cells within the root meristem into a distal fate. To test this prediction, we created an inducible line by fusing NTT to the glucocorticoid receptor (p35S-NTT-GR) (*16*). In the wild type, columella cells are restricted to the distal region within the root meristem. In contrast, induction of NTT activity within mature root meristems caused ectopic production of columella cells (Fig. 4, A and B). The QC25 marker, normally expressed only in the quiescent center, was ectopically expressed in the proximal region when NTT activity was induced. Thus, NTT is both necessary and sufficient to pattern distal stem cell identity within the root meristem. The p35S-NTT-GR line can also mimic the root-inducing effects of exogenous auxin application. When WT seedlings were transferred to normal media after germinating on 10-μm 1-naphthaleneacetic acid (NAA), extra roots were produced. Similarly, extra roots formed after p35S-NTT-GR seeds were germinated in the presence of the dexamethasone inducer and then transferred to normal media (fig. S8). This is consistent with a role of the *NWW* genes in mediating an auxin signal for root initiation.

NTT misexpression can also change stem cell fate within the embryo. In WT embryos, the apical region gives rise to the shoot apical meristem and two groups of primordial cells known as the cotyledon initials. The *AS1* gene is strongly expressed in the cotyledon initials in transition-stage embryos (*17*). Misexpression of *NTT* under the control of the *AS1* promoter caused roots to form instead of cotyledons in the resultant seedlings (Fig. 4, C and D, and fig. S8, E to G). This suggests that *NTT* expression is sufficient to transform cotyledon primordia to a root meristem fate within the apical region of the embryo.

More widespread *NTT* misexpression in the protodermal layer of the apical cells of early globular-stage embryos using the AtML1 promoter (pML1>>NTT) (*18*) resulted in embryos with asymmetrical structure, losing both the cotyledons and the shoot apical meristem (Fig. 4, E and F, and fig S8). Taken together, these studies support a model in which *NTT* misexpression is sufficient to pattern basal stem cell identity within the embryo and distal stem cell identity in the root meristem (fig. S8K).

There is tremendous interest in identifying the major pathways that specify stem cells in both animal and plant systems. Identification of the *NWW* genes will help to explain the formation of stem cells and may ultimately allow for the manipulation of the root to enhance agricultural yield. Additionally, although many regulators have been found to pattern plant meristems, it is likely that additional intrinsic factors remain undiscovered due to genetic redundancy, as is the case with the *NWW* genes.

REFERENCES AND NOTES

1. T. Bennett, B. Scheres, in *Plant Development*, M. C. P. Timmermans, Ed. (Academic Press, San Diego, CA, 2010), pp. 67–102.
2. B. Scheres, P. Benfey, L. Dolan, in *The Arabidopsis Book*, C. R. Somerville, E. M. Meyerowitz, Eds. (American Society of Plant Biologists, Rockville, MD, 2002), pp. 1–18.
3. B. C. Crawford, M. F. Yanofsky, *Curr. Biol.* **18**, R972–R978 (2008).
4. B. C. Crawford, G. Ditta, M. F. Yanofsky, *Curr. Biol.* **17**, 1101–1108 (2007).
5. M. Sagasser, G. H. Lu, K. Hahlbrock, B. Weisshaar, *Genes Dev.* **16**, 138–149 (2002).
6. S. Warming, N. Costantino, D. L. Court, N. A. Jenkins, N. G. Copeland, *Nucleic Acids Res.* **33**, e36 (2005).
7. Y. G. Liu *et al.*, *Proc. Natl. Acad. Sci. U.S.A.* **96**, 6535–6540 (1999).
8. C. S. Hardtke, T. Berleth, *EMBO J.* **17**, 1405–1411 (1998).
9. J. Friml *et al.*, *Nature* **426**, 147–153 (2003).
10. J. Friml *et al.*, *Cell* **108**, 661–673 (2002).
11. D. Weijers *et al.*, *Plant Cell* **17**, 2517–2526 (2005).
12. D. Weijers *et al.*, *Dev. Cell* **10**, 265–270 (2006).
13. A. K. Sarkar *et al.*, *Nature* **446**, 811–814 (2007).
14. T. Berleth, G. Jurgens, *Development* **118**, 575–587 (1993).
15. C. van den Berg, V. Willemsen, G. Hendriks, P. Weisbeek, B. Scheres, *Nature* **390**, 287–289 (1997).
16. T. Aoyama, N. H. Chua, *Plant J.* **11**, 605–612 (1997).
17. M. E. Byrne *et al.*, *Nature* **408**, 967–971 (2000).
18. A. Sessions, D. Weigel, M. F. Yanofsky, *Plant J.* **20**, 259–263 (1999).

ACKNOWLEDGMENTS

We thank A. Gallavotti and B. Bargmann for their critical comments and M. Estelle and Y. Zhang for use and help with the confocal microscope. This work was funded by the NSF (grants IOS-0817544 and IOS-1121055 to M.F.Y. and IOS-0822411 to J.A.L.) and the NIH (NIH/NIGMS grant 5 R01 GM072764 to J.A.L.).
The supplementary materials contain additional data.

SUPPLEMENTARY MATERIALS

www.sciencemag.org/content/347/6222/655/suppl/DC1
Materials and Methods
Figs. S1 to S8
Table S1
References (*19*–*29*)

8 October 2014; accepted 9 January 2015
Published online 22 January 2015;
10.1126/science.aaa0196

ADDICTION THERAPY

Refining deep brain stimulation to emulate optogenetic treatment of synaptic pathology

Meaghan Creed,[1] Vincent Jean Pascoli,[1] Christian Lüscher[1,2]*

Circuit remodeling driven by pathological forms of synaptic plasticity underlies several psychiatric diseases, including addiction. Deep brain stimulation (DBS) has been applied to treat a number of neurological and psychiatric conditions, although its effects are transient and mediated by largely unknown mechanisms. Recently, optogenetic protocols that restore normal transmission at identified synapses in mice have provided proof of the idea that cocaine-adaptive behavior can be reversed in vivo. The most efficient protocol relies on the activation of metabotropic glutamate receptors, mGluRs, which depotentiates excitatory synaptic inputs onto dopamine D1 receptor medium-sized spiny neurons and normalizes drug-adaptive behavior. We discovered that acute low-frequency DBS, refined by selective blockade of dopamine D1 receptors, mimics optogenetic mGluR-dependent normalization of synaptic transmission. Consequently, there was a long-lasting abolishment of behavioral sensitization.

Deep brain stimulation (DBS) consists of passing electric current, typically in excess of 100 Hz, through electrodes surgically implanted into subcortical nuclei of the brain. DBS is currently an FDA-approved treatment for Parkinson's disease, dystonia, and essential tremor (*1*, *2*). Additional indications, such as depression, obsessive-compulsive disorders, and addiction have been considered (*3*). The mechanisms by which DBS produces its therapeutic effects remain largely unknown (*4*, *5*), although recent studies suggest that it may have widespread effects on brain network activity (*6*, *7*). In the context of addictive disorders, altered activity in areas projecting to the nucleus accumbens (NAc), such as the medial prefrontal cortex (mPFC), has been implicated in the effects of DBS (*8*). The effects of classical high-frequency DBS are transient. Symptoms

[1]Department of Basic Neurosciences, University of Geneva, Geneva, Switzerland. [2]Service of Neurology, Department of Clinical Neurosciences, University Hospital of Geneva, Geneva, Switzerland.
*Corresponding author. E-mail: christian.luscher@unige.ch

typically reappear once stimulation is stopped, requiring lifelong continuous stimulation (*9*). Because pathological synaptic plasticity drives circuit dysfunction in many neurological and psychiatric disorders (*10*, *11*), tailoring DBS to restore normal transmission may have long-lasting effects and thus represent a major therapeutic advance.

Addiction may be a condition ideally suited to test the potential of DBS to correct pathological synaptic function, because the disease is associated with behavioral changes (*12*) that are caused by drug-evoked synaptic plasticity of glutamatergic transmission in the mesolimbic dopamine system (*13*, *14*). Specifically, in the NAc, cocaine exposure increases the strength of excitatory afferents onto dopamine D1 receptor–expressing medium-sized spiny neurons (D1R MSNs) (*15*, *16*). This plasticity underlies behavioral changes associated with drugs of abuse, such as psychomotor sensitization (*15*, *17*). Low-frequency optogenetic stimulation of the excitatory projections to the NAc is able to reverse cocaine-evoked plasticity and erase drug-adaptive behaviors (*15*, *18*).

Locomotor sensitization is a straightforward behavioral paradigm used to model drug-adaptive behavior (*19*, *20*). In rodents, repeated cocaine exposure induces progressively enhanced locomotor activation in response to a cocaine injection; after five injections, the locomotor response is typically fully sensitized, a state that persists for months after cocaine withdrawal (*21*). Locomotor sensitization is thus thought to underlie important aspects of vulnerability to drug addiction and relapse, specifically drug craving (*19*, *21*, *22*). The expression of locomotor sensitization is mediated by enhanced glutamatergic transmission in the NAc (*23*–*25*). After repeated cocaine exposure, glutamate projections selectively onto D1R MSNs of the NAc are strengthened (*15*, *26*), which is driven by the insertion of AMPA receptors (*27*–*29*).

As expected, sequential injections of cocaine in mice [20 mg per kilogram of body weight (mg/kg), intraperitoneally (i.p.)] progressively enhanced the locomotor response, which plateaued after five sequential injections and was still elevated during the cocaine challenge test, given after 10 days of withdrawal (Fig. 1A). Classical high-frequency DBS (130 Hz, 90 μs) applied to the shell of the NAc (Fig. 1B and fig. S1) during the cocaine challenge suppressed the sensitization, but had no effect on the acute locomotor response to cocaine in saline controls (Fig. 1C). When DBS was applied to the NAc shell for 60 min leading up to the cocaine

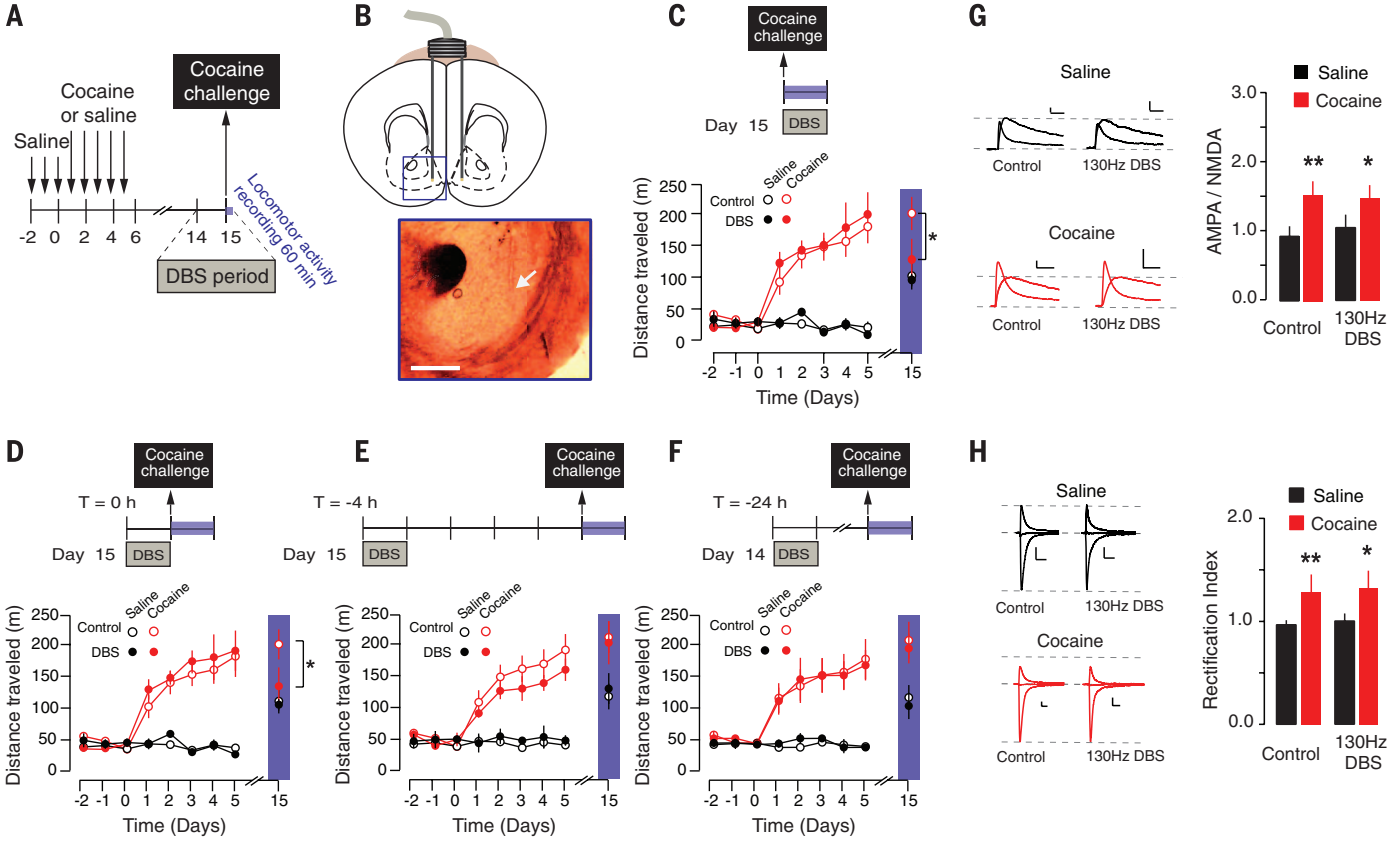

Fig. 1. Classical DBS transiently suppresses locomotor sensitization to cocaine and fails to depotentiate excitatory transmission onto D1R MSNs. (**A**) Schematic of experiment: Cocaine locomotor activity is monitored for 60 min, immediately after the injection of cocaine or saline. (**B**) Coronal section depicting bilateral electrode placement in the anterior portion of the NAc shell. Scale bar, 250 μM. (**C**) After five daily cocaine injections, a robust locomotor sensitization is observed that persists for 10 days after withdrawal; 130-Hz DBS applied during the cocaine challenge on day 15 reduced the locomotor sensitized response [controls: saline/cocaine = 10/10; 130-Hz DBS: saline/cocaine = 8/8. Repeated measures analysis of variance (ANOVA) with post-hoc *t* test; cocaine control versus cocaine 130-Hz DBS, $t = 2.27$, $P = 0.035$]. (**D**) 130-Hz DBS applied immediately before cocaine challenge [time (T) = 0 hours] also suppressed the sensitized response to cocaine (controls: saline/cocaine = 9/14, $T = 0$ hours; 130-Hz DBS: saline/cocaine = 5/9. Repeated measures ANOVA with post-hoc *t* test; cocaine control versus cocaine 130-Hz DBS, $t = 2.19$, $P = 0.041$). (**E**) 130-Hz DBS did not have an effect on the sensitized response to cocaine when applied 4 hours ($T = 4$ hours, 130-Hz DBS: saline/cocaine = 6/8) and (**F**) 24 hours ($T = 24$ hours, 130-Hz DBS: saline/cocaine = 5/8) before cocaine challenge. (**G**) Cocaine treatment significantly increased the AMPA/NMDA ratio (controls: saline/cocaine = 8/7; 130-Hz DBS: saline/cocaine = 7/7. Two-way ANOVA with post-hoc *t* test, saline versus cocaine control, $t = 2.34$, $P = 0.036$, saline 130-Hz DBS versus cocaine 130-Hz DBS, $t = 2.23$, $P = 0.049$). (**H**) Cocaine treatment also significantly increased the rectification index (controls: saline/cocaine = 7/6; 130-Hz DBS: saline/cocaine = 7/7. Two-way ANOVA with post-hoc *t* test, saline versus cocaine control, $t = 2.39$, $P = 0.034$; saline 130-Hz DBS versus cocaine 130-Hz DBS, $t = 2.21$, $P = 0.050$) measured in D1R MSNs; 130-Hz DBS had no effect on either parameter. Representative traces of control animals (left) and animals treated with 130-Hz DBS (right) are shown. Saline-treated animals are shown in black and cocaine-treated animals in red. Scale bars are 20 pA and 20 ms. All plots are means with SEM, $^*P < 0.05$, $^{**}P < 0.01$.

challenge, locomotor sensitization was still suppressed (Fig. 1D and fig. S2, A and B). This suppression was not observed when DBS was applied to the mPFC (fig. S2C) or the core of the NAc (fig. S2D). However, when the interval between DBS offset and cocaine challenge was extended to 4 hours (Fig. 1E) or 24 hours (Fig. 1F), the sensitized response was not reduced, relative to unstimulated controls. High-frequency DBS had no effect on general ambulatory activity, as measured by an open-field task (fig. S3A). Classical high-frequency DBS thus has only a transient effect on behavioral sensitization, probably because this manipulation does not affect cocaine-evoked synaptic plasticity.

As in previous studies (*15*), cocaine led to a long-lasting strengthening of excitatory transmission onto D1R MSNs (Fig. 1G), which were identified by using BAC transgenic mice expressing a reporter protein (td-Tomato) under the control of a *drd1a* promoter. This potentiation was determined by measuring an increase of the ratio of AMPA receptor (AMPAR) excitatory postsynaptic potentials (EPSCs) over *N*-methyl-D-aspartate receptor (NMDAR) EPSCs (the AMPA/NMDA ratio). In addition, we observed an inward rectification of AMPAR currents (Fig. 1H). This inward rectification is indicative of GluA2-lacking AMPARs. Their insertion also contributes to increases in synaptic strength (*30*–*32*). Viral insertion of GluA2-lacking AMPARs into the NAc is indeed sufficient to induce sensitization (*33*). Neither of these indices of cocaine-evoked plasticity was affected by the 130-Hz DBS applied 24 hours before the ex vivo recordings (Fig. 1, G and H).

Why was high-frequency DBS unable to restore normal synaptic transmission in the NAc? To reverse cocaine-evoked potentiation, one would have to apply a depotentiation or long-term depression (LTD) protocol. Stimulation frequencies at very high frequencies (>100 Hz) are unlikely to induce a LTD [previous studies have actually shown an induction of long-term potentiation (LTP) (*34*, *35*)] of excitatory transmission. However, in the NAc, low-frequency (10 to 15 Hz) stimulation elicits a LTD that depends on mGluRs and also efficiently removes GluA2-lacking AMPARs (*36*). We therefore directly compared the magnitude of synaptic depression induced by optogenetic and electrical stimulation delivered at 12 Hz in slices obtained from cocaine-treated drd1a-td-tomato mice (Fig. 2, A and B). For these proof-of-concept experiments, we used one injection of cocaine 7 days before the electrophysiological recordings or the cocaine challenge, a protocol that efficiently potentiates D1R MSN afferents and induces sensitization (*15*). We injected ChR2 tagged with enhanced yellow fluorescent protein (eYFP) into the mPFC of drd1a-td-tomato mice (fig. S4A) and cut slices of the NAc after 5 to 8 weeks of expression (see the supplementary materials). Ex vivo, 473-nm light stimulation at 12 Hz induced a robust LTD of excitatory transmission onto D1R MSNs (Fig. 2C), whereas this same protocol applied with electrical stimulation failed to do so (Fig. 2D, open circles). Because previous studies have indicated that blockade of D1Rs is necessary to unmask the mGluR-dependent LTD in D1R MSNs (*37*), we repeated the electrical stimulation in the presence of the D1R antagonists SCH23390 (10 μM) or SCH39166 (10 μM). In the presence of either compound, we observed an LTD comparable to that observed with optogenetic stimulation (Fig. 2D and fig. S5A).

Using the insight gained from these ex vivo LTD experiments, we sought to design a rational DBS protocol for use in vivo. Using a two-injection

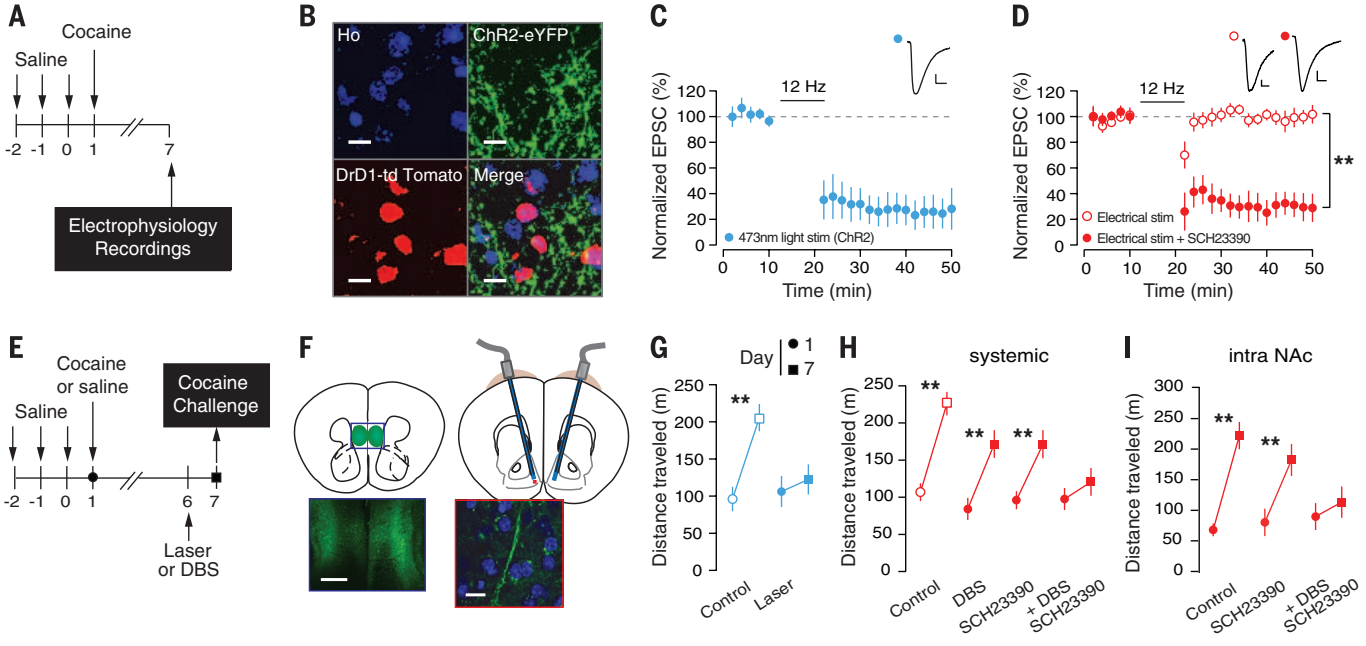

Fig. 2. Optogenetically inspired DBS reverses locomotor sensitization to cocaine and induces LTD in vitro, in the presence of a D1 antagonist. (**A**) Schematic of the experiment. (**B**) Confocal image with DAPI staining of ChR2 fibers tagged with eYFP in the NAc shell in a D1R-td-tomato mouse (scale bar, 20 μM). (**C**) A robust (−61.2%) LTD of EPSC was induced by 12-Hz laser stimulation in D1R MSNs (n = 10, t test with paired samples, mean baseline versus mean post-HFS, t = 4.68, P < 0.001). Inset: Representative trace at baseline (black) and after 12-Hz stimulation (blue); scale bar, 5 ms, 10 pA. Symbols represent the average of 12 trials. (**D**) LTD of EPSC measured in D1R MSNs was not induced by 12-Hz electrical stimulation in control conditions (open circles) but was unmasked in the presence of SCH23390 (−65.17%, solid circles). Inset: Representative traces in the absence (left) and presence (right) of SCH23390 at baseline (black) and after 12-Hz stimulation (red); scale bar, 5 ms, 10 pA; left, control; right, SCH23390 (control/SCH23390 = 6/7, repeated measures ANOVA, T × SCH23390, F = 8.50, P < 0.001). (**E**) Schematic of in vivo experiments. (**F**) Diagram of channelrhodopsin infection site (mPFC; scale bar, 200 μM) with optic fibers implanted in the NAc shell (scale bar, 20 μM). (**G**) Sensitization was abolished by 12-Hz optogenetic stimulation in vivo (control n = 9, laser n = 9; t = 2.73, P = 0.015). (**H**) Sensitization was significantly reduced by 12-Hz DBS in combination with SCH23390, but not by either intervention alone (control n = 11, SCH23390 n = 9, 12-Hz DBS n = 12, DBS + SCH23390 n = 12, ANOVA with t test: control versus SCH23390 + 12-Hz DBS, t = 2.98, P = 0.007, SCH23390 versus SCH23390 + 12-Hz DBS, t = 2.63, P = 0.016, 12-Hz DBS versus SCH23390 + 12 -z DBS, t = 2.23, P = 0.034). (**I**) Sensitization was significantly reduced when SCH23390 was infused into the NAc shell in combination with 12-Hz DBS (control = 11, SCH23390 intraNAc + 12-Hz DBS = 12, t = 3.00, P = 0.007), but not by infusion of SCH23390 alone (n = 12, control versus SCH23390 intraNAc, t = 0.93, P = 0.363). All plots are means with SEM, *P < 0.05, **P < 0.01.

sensitization paradigm, we determined that 12-Hz in vivo optogenetic stimulation (Fig. 2, E and F, and fig. S4B) applied bilaterally to the NAc 24 hours before the cocaine challenge abolished the sensitized locomotor response (Fig. 2G). Neither 12-Hz DBS alone nor SCH23390 (0.3 mg/kg, i.p.) administered alone affected sensitization, but when given in combination, sensitization was abolished when challenged 24 hours later (Fig. 2H). To confirm that local blockade of D1Rs is necessary for the effects of 12-Hz DBS, we infused SCH23390 (0.15 μg in 300 nl) bilaterally into the NAc shell. This infusion, in combination with 12-Hz DBS, was sufficient to abolish sensitization, confirming the important role of the antagonism of D1R specifically in the NAc (Fig. 2I). None of the above interventions affected spontaneous locomotor activity (fig. S3, B and C).

To establish a causal link between cocaine-evoked synaptic plasticity and the abolition of fully established locomotor sensitization, we evaluated

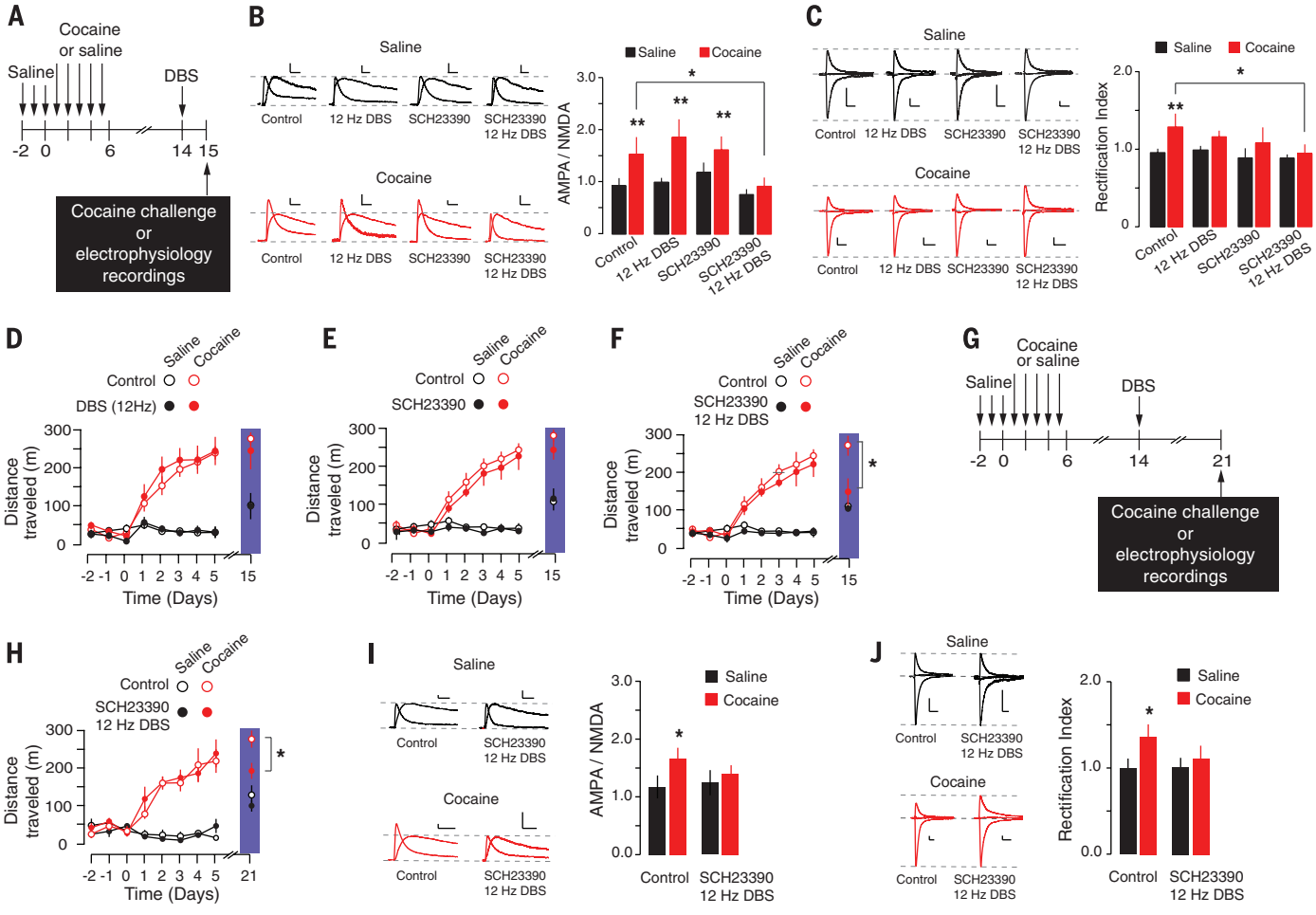

Fig. 3. Optogenetically inspired DBS reverses locomotor sensitization to cocaine and cocaine-evoked plasticity in D1R MSNs. (**A**) Schematic of experiment. (**B**) Representative traces and summary plot of AMPA/NMDA (n = 6 to 8 cells per condition). There was a significant effect of cocaine (ANOVA, cocaine effect F_1 = 10.76, P = 0.002) and a significant interaction between DBS and SCH23390 treatment (F_1 = 5.74, P = 0.020) on the AMPA/NMDA ratio. AMPA/NMDA in cocaine-treated animals treated with DBS was reduced to the level of that in saline-treated controls (cocaine control versus cocaine + DBS, t = 2.39, P = 0.029). Sample traces are of AMPA and NMDA EPSCs at +40 mV from saline- (black) and cocaine-treated (red) animals. (**C**) Representative traces and summary plot of rectification index (n = 6 to 8 cells per condition). There was a significant effect of cocaine on RI (ANOVA, cocaine effect F_1 = 6.04, P = 0.018); cocaine-treated animals that had undergone DBS were not different from saline-treated controls (cocaine control versus cocaine + DBS, t = 2.16, P = 0.046). Sample traces are of AMPAR EPSCs at −70, 0, and +40 mV from saline- (black) and cocaine-treated (red) animals. (**D**) 12-Hz DBS alone (controls: saline/cocaine = 9/10, 12-Hz DBS: saline/cocaine = 6/8) or (**E**) SCH23390 alone (controls: saline/cocaine = 9/9; SCH23390: saline/cocaine = 5/7) did not affect sensitization to cocaine. (**F**) 12-Hz DBS in combination with SCH23390 reduced the sensitized locomotor response to cocaine (controls: saline/cocaine = 9/10; DBS: saline/cocaine = 11/8, post-hoc t test on cocaine challenge: cocaine control versus cocaine 12-Hz DBS, t = 2.98, P = 0.008); there was a significant effect of cocaine (repeated measures ANOVA, F_1 = 30.72, P <0.001) and interaction between time and DBS (F_5 = 17.48, P < 0.001) and interaction between cocaine and treatment (F_5 = 2.707, P = 0.022, post-hoc t test on cocaine challenge: cocaine control versus cocaine DBS, t = 2.98, P = 0.008). (**G**) Experimental protocol. (**H**) Locomotor response to cocaine was suppressed 7 days after DBS with SCH23390 (controls: saline/cocaine = 4/6; DBS + SCH23390: saline/cocaine = 6/10, cocaine control versus cocaine + SCH23390 and DBS, t = 2.59, P = 0.021). (**I**) Representative traces and summary plot of AMPA/NMDA (n = 7 to 12 cells per condition). AMPA/NMDA in cocaine-treated animals treated with DBS was reduced to the level of saline-treated controls (cocaine control versus cocaine + SCH23390 DBS, t = 2.35, P = 0.029). Sample traces are of AMPA and NMDA EPSCs at +40 mV from saline- (black) and cocaine-treated (red) animals. (**J**) Representative traces and summary plot of rectification index (n = 6 to 9 cells per condition). Cocaine-treated animals that had undergone DBS were not different from saline-treated controls (cocaine control versus cocaine + DBS, t = 2.02, P = 0.062). Sample traces are of AMPAR EPSCs at −70, 0, and +40 mV from saline- (black) and cocaine-treated (red) animals. Scale bars, 20 pA and 20 ms. *P < 0.05, **P < 0.01.

the effects of LTD on synaptic transmission by returning to the five-injection sensitization protocol. Mice underwent 5 days of cocaine treatment, and electrophysiological recordings were performed after 10 days of withdrawal (Fig. 3A and fig. S5B). In control animals, cocaine treatment led to an increase in the AMPA/NMDA ratio and rectification index (Fig. 3, B and C, and fig. S4C). 12-Hz DBS, when applied in combination with the D1R antagonist, normalized these parameters, but 12-Hz DBS or D1R antagonist applied separately failed to do so (Fig. 3, B and C, and fig. S5, C and D). Accordingly, in the five-injection sensitization protocol, 12-Hz DBS alone (Fig. 3D) or SCH23390 alone (Fig. 3E) had no effect on sensitization, whereas SCH23390 or SCH39166 in combination with DBS significantly reduced the sensitization, without affecting the acute response to cocaine (Fig. 3F and fig. S5E). There was a trend toward a decrease in the RI with SCH23390, which could be due to an endogenous activation of mGluR signaling. In the case of 12-Hz DBS alone, the strong mGluR activation may partially overcome inhibition by D1R signaling. However, these effects were not significant, and there was no effect of either intervention on locomotor sensitization.

These results were comparable in magnitude to the effects of 12-Hz optogenetic stimulation on the sensitized response to cocaine and cocaine-evoked plasticity in the same five-injection protocol (fig. S6, A to D). Furthermore, we confirmed that the sensitized locomotor response to cocaine was still present 2 weeks after cocaine exposure (Fig. 3G), and we demonstrated that the sensitized locomotor response was still suppressed when DBS in combination with SCH23390 was given 1 week before the challenge. Cocaine-evoked plasticity was also still normalized at this time point (Fig. 3, I and J). These results strengthen the observation that the acute intervention has long-lasting effects on both cocaine-evoked plasticity and consequent locomotor sensitization.

There are two general classes of LTD available in MSNs of the NAc. mGluR-dependent LTD is induced at frequencies between 10 and 15 Hz, whereas a second form depends on NMDAR activation and is induced by stimulation at lower frequencies (~1 Hz) (*38*–*40*). Given that DBS was delivered at 12 Hz, a mGluR-dependent mechanism seems likely. In a final series of experiments, we confirmed the crucial role of mGluR1 in the effects of DBS in combination with SCH23390. Mice pretreated with the selective mGluR1 antagonist A-841720 (0.1 mg/kg, i.p.) were not sensitive to the effects of SCH23390 in combination with 12-Hz DBS, in reversing both locomotor sensitization (Fig. 4A) and cocaine-evoked plasticity (Fig. 4B). Conversely, pretreatment with NMDAR antagonist MK-801 (0.2 mg/kg, i.p.) had no effect on the efficacy of SCH23390 in combination with 12-Hz DBS (Fig. 4, C and D). Again, no intervention tested affected acute locomotor activity (fig. S2D). To further highlight the crucial role of the mGluR1 receptor in the depotentiation mechanism induced by DBS, we first showed that the activation of mGluR1 by dihydroxyphenylglycine (DHPG) in presence of the mGluR5 antagonist MPEP (see

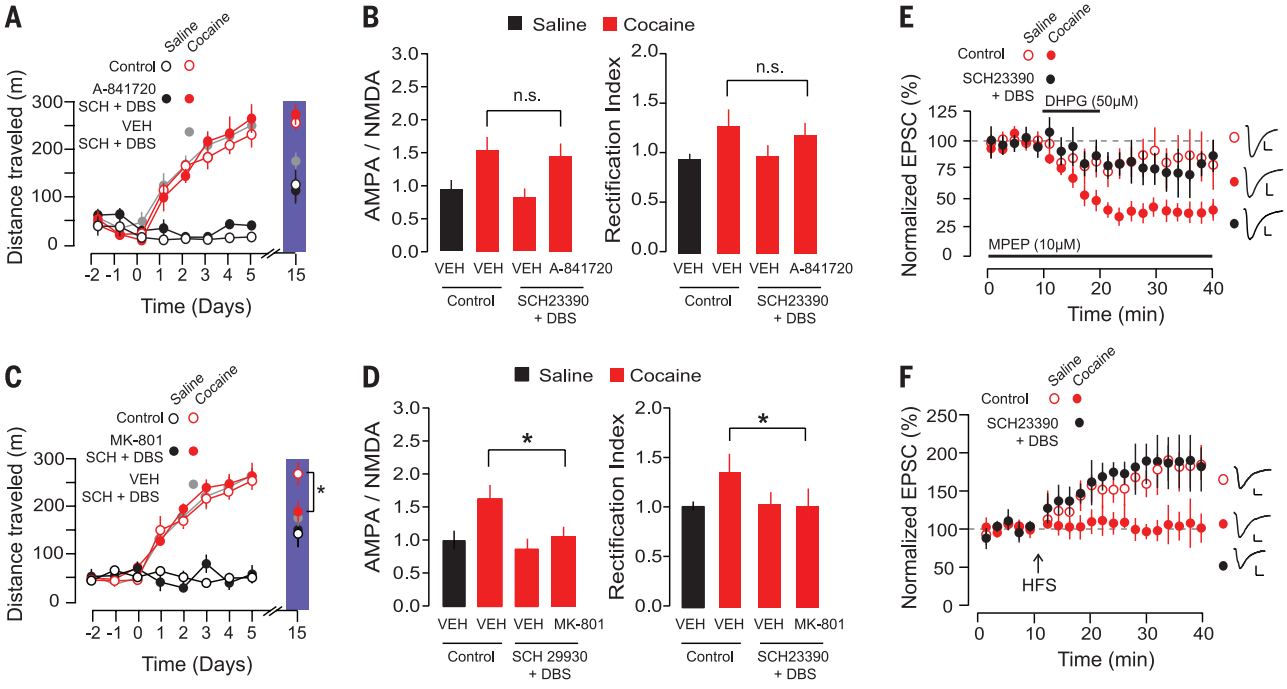

Fig. 4. Optogenetically inspired DBS exerts its effects via an mGluR-dependent mechanism. (**A**) Pretreatment with the mGluR1 antagonist A-841720 prevented the reversal of sensitized locomotor response (controls: saline/cocaine = 7/12; A-841720 with SCH23390 + 12-Hz DBS: saline/cocaine = 4/6) and (**B**) reversal of increased AMPA/NMDA and rectification index (AMPA/NMDA: controls: saline/cocaine = 8/7; cocaine with SCH23390 + 12-Hz DBS with/without A-841720 pretreatment = 11/12. Rectification index: controls: saline/cocaine = 6/7; cocaine with OiDBS with/without A-841720 pretreatment = 8/11) induced by SCH23390 + 12-Hz DBS in cocaine-treated animals. (**C**) MK-801 did not alter the ability of SCH23390 + 12-Hz DBS to reverse locomotor sensitization (controls: saline/cocaine = 7/6; A-841720 with SCH23390 + 12-Hz DBS: saline/cocaine = 5/5) or (**D**) cocaine-evoked increases in the AMPA/NMDA (left) or rectification index (right). (**E**) A slight LTD of EPSCs in D1R MSNs was induced by DHPG (50 μM) in saline-treated animals (−22.67% ± 18.74), which was greater in cocaine-treated animals (−68.26%, ± 16.14), after incubation with MPEP. This DHPG-induced LTD was occluded in cocaine-treated animals that underwent SCH23390 + 12-Hz DBS (−19.65% ± 15.52. Controls: saline/cocaine = 9/12; cocaine with SCH23390 + 12-Hz DBS = 8. Repeated measures ANOVA, treatment effect $F_2 = 5.92$, $P = 0.008$; Bonferroni post-hoc test, saline versus cocaine $P = 0.006$, saline versus cocaine and SCH23390 + 12-Hz DBS, $P = 0.939$). Inset: Representative traces at baseline (black) and 20 min after protocol (red) in saline-treated mice (top), cocaine-treated mice (center), and cocaine-treated mice that underwent SCH23390 + 12-Hz DBS 24 hours before being killed (bottom). Scale bar = 10 pA, 50 ms. (**F**) HFS induced an LTP of EPSCs in D1R MSNs in saline-treated animals (89.37%, ± 21.31), but was occluded in cocaine-treated animals (−7.64%, ± 15.132) (controls: saline/cocaine = 9/7, repeated measures ANOVA, effect of treatment $F_2 = 9.016$, $P = 0.002$; Bonferroni post-hoc test, saline versus cocaine, $P = 0.987$). LTP in cocaine-treated mice was rescued by treatment with SCH23390 + 12-Hz DBS (110.49%, ± 29.87; $n = 6$, $P = 0.004$), Inset: Representative traces at baseline (black) and 20 min afte protocol (red), in saline-treated mice (top), cocaine-treated mice (center), and cocaine-treated mice that underwent SCH23390 + 12-Hz DBS (bottom). Scale bars, 10 pA, 50 ms.

methods) induced a LTD of excitatory transmission onto D1R MSNs (Fig. 4E). Consistent with previous studies, the magnitude of this LTD was enhanced in cocaine-treated as compared to saline-treated animals (*41, 42*). However, in cocaine-treated animals that underwent SCH23390 exposure in combination with 12-Hz DBS 24 hours before being killed, this enhanced mGluR1 LTD was occluded, suggesting a shared mechanism between DBS and DHPG-induced LTD. Finally, cocaine exposure occludes the ability of high-frequency stimulation (HFS) to induce a LTP in D1R MSNs (*15*). SCH23390 in combination with 12-Hz DBS rescued HFS LTP in cocaine treated animals, further suggesting that DBS induces a depotentiation in vivo (Fig. 4F).

We used insight obtained from optogenetic in vivo manipulations to propose a novel DBS protocol, which efficiently abolishes behavioral sensitization to cocaine through the reversal of cocaine-evoked potentiation of excitatory transmission onto D1R MSNs. Classical high-frequency DBS does not alter cocaine-evoked plasticity and has only transient effects on locomotor sensitization; its behavioral effects are mediated through a mechanism that remains elusive. Low-frequency DBS applied on its own fails to affect drug-evoked plasticity, most likely because it causes release from dopamine terminals, due to the nonspecific nature of electrical stimulation. Only the combination of acute low-frequency DBS with a D1R antagonist (optogenetically inspired DBS) then enables the induction of the mGluR1 LTD necessary for the depotentation of synapses on D1R MSNs, most likely formed by the projections from the mPFC (*18*), and abolishment of the drug-adaptive behavior. Given that SCH39166 is a U.S. Food and Drug Administration–approved D1R antagonist (*43*), translational studies in humans may be feasible.

Our results demonstrate the potential of novel DBS protocols inspired by optogenetic manipulations of synaptic pathology. Using DBS to correct synaptic pathology and restore normal behavior may have applications in other neuropsychiatric disorders. Given the obstacles to the rapid translation of optogenetic interventions to humans (*44*), these findings may lead to a full realization of the potential of novel DBS protocols.

REFERENCES AND NOTES

1. A. L. Benabid *et al.*, *Lancet* **337**, 403–406 (1991).
2. S. Miocinovic, S. Somayajula, S. Chitnis, J. L. Vitek, *J. Am. Med. Assoc. Neurol.* **70**, 163–171 (2013).
3. N. R. Williams, M. S. Okun, *J. Clin. Invest.* **123**, 4546–4556 (2013).
4. H. J. Heinze *et al.*, *Front. Hum. Neurosci.* **3**, 22 (2009).
5. U. J. Müller *et al.*, *Ann. N. Y. Acad. Sci.* **1282**, 119–128 (2013).
6. P. J. Hahn, C. C. McIntyre, *J. Comput. Neurosci.* **28**, 425–441 (2010).
7. M. S. Okun, *N. Engl. J. Med.* **28**, 425–441 (2010).
8. F. M. Vassoler *et al.*, *J. Neurosci.* **33**, 14446–14454 (2013).
9. K. A. Follett, *Annu. Rev. Med.* **51**, 135–147 (2000).
10. A. F. Arnsten, K. Rubia, *J. Am. Acad. Child Adolesc. Psychiatry* **51**, 356–367 (2012).
11. K. Deisseroth, *Nature* **505**, 309–317 (2014).
12. G. F. Koob, N. D. Volkow, *Neuropsychopharmacology* **35**, 217–238 (2010).
13. M. C. Creed, C. Lüscher, *Curr. Opin. Neurobiol.* **23**, 553–558 (2013).
14. C. Lüscher, R. C. Malenka, *Neuron* **69**, 650–663 (2011).
15. V. Pascoli, M. Turiault, C. Lüscher, *Nature* **481**, 71–75 (2011).
16. A. F. MacAskill, J. M. Cassel, A. G. Carter, *Nat. Neurosci.* **17**, 1198–1207 (2014).
17. G. Di Chiara, V. Bassareo, *Curr. Opin. Pharmacol.* **7**, 69–76 (2007).
18. V. Pascoli *et al.*, *Nature* **509**, 459–464 (2014).
19. T. E. Robinson, K. C. Berridge, *Addiction* **96**, 103–114 (2001).
20. E. Valjent *et al.*, *Neuropsychopharmacology* **35**, 401–415 (2010).
21. T. E. Robinson, K. C. Berridge, *Brain Res. Brain Res. Rev.* **18**, 247–291 (1993).
22. J. D. Steketee, P. W. Kalivas, *Pharmacol. Rev.* **63**, 348–365 (2011).
23. M. S. Reid, S. P. Berger, *Neuroreport* **7**, 1325–1329 (1996).
24. Y. Li, M. E. Wolf, F. J. White, *Behav. Brain Res.* **104**, 119–125 (1999).
25. P. W. Kalivas, B. Weber, *J. Pharmacol. Exp. Ther.* **245**, 1095–1102 (1988).
26. J. P. Britt *et al.*, *Neuron* **76**, 790–803 (2012).
27. A. C. Boudreau, M. E. Wolf, *J. Neurosci.* **25**, 9144–9151 (2005).
28. K. L. Conrad *et al.*, *Nature* **454**, 118–121 (2008).
29. L. J. Vanderschuren, P. W. Kalivas, *Psychopharmacology (Berlin)* **151**, 99–120 (2000).
30. E. S. Guire, M. C. Oh, T. R. Soderling, V. A. Derkach, *J. Neurosci.* **28**, 6000–6009 (2008).
31. S. Q. Liu, S. G. Cull-Candy, *Nature* **405**, 454–458 (2000).
32. K. Plant *et al.*, *Nat. Neurosci.* **9**, 602–604 (2006).
33. W. A. Carlezon Jr. *et al.*, *Science* **282**, 2272–2275 (1998).
34. S. M. Schotanus, K. Chergui, *Eur. J. Neurosci.* **27**, 1957–1964 (2008).
35. E. Cahill *et al.*, *Mol. Psychiatry* **19**, 1295–1304 (2014).
36. C. C. Huang *et al.*, *J. Neurosci.* **31**, 4194–4203 (2011).
37. W. Shen, M. Flajolet, P. Greengard, D. J. Surmeier, *Science* **321**, 848–851 (2008).
38. S. Thomas *et al.*, *Philos. Trans.R. Soc. London Ser. B* **358**, 815–819 (2003).
39. D. Robbe, M. Kopf, A. Remaury, J. Bockaert, O. J. Manzoni, *Proc. Natl. Acad. Sci. U.S.A.* **99**, 8384–8388 (2002).
40. C. Lüscher, R. C. Malenka, *Cold Spring Harb. Perspect. Biol.* **4**, 1–15 (2012).
41. J. E. McCutcheon *et al.*, *J. Neurosci.* **31**, 14536–14541 (2011).
42. M. E. Wolf, K. Y. Tseng, *Front. Mol. Neurosci.* **5**, 72 (2012).
43. R. C. Pierce, C. P. O'Brien, P. J. Kenny, L. J. Vanderschuren, *Cold Spring Harb. Perspect. Med.* **2**, 1–8 (2012).
44. B. Y. Chow, E. S. Boyden, *Sci. Transl. Med.* **5**, 177ps5 (2013).

ACKNOWLEDGMENTS

Funding was provided by the Swiss National Science Foundation, the National Competence Center for Research Synapsy, the European Brain Council (Advanced grant MeSSI), the Carigest Foundation, the Academic Society of Geneva, and the Fondation Divesa Foundation. We thank P. Pollak, D. Jabaudon, E. O'Connor, and A. Holtmaat for feedback on the manuscript and members of the Lüscher lab for stimulating discussions. Data sets presented in this study are available at the University of Geneva open access data archive (www.archive-ouverte.unige.ch) with accession number 18515.

SUPPLEMENTARY MATERIALS

www.sciencemag.org/content/347/6222/659/suppl/DC1
Materials and Methods
Figs. S1 to S6
Table S1
References (*45–49*)

3 September 2014; accepted 8 January 2015
10.1126/science.1260776

GENOMIC VARIATION

Impact of regulatory variation from RNA to protein

Alexis Battle,[1,2]*‡ Zia Khan,[3]†‡ Sidney H. Wang,[3]‡ Amy Mitrano,[3] Michael J. Ford,[4] Jonathan K. Pritchard,[1,2,5]§ Yoav Gilad[3]§

The phenotypic consequences of expression quantitative trait loci (eQTLs) are presumably due to their effects on protein expression levels. Yet the impact of genetic variation, including eQTLs, on protein levels remains poorly understood. To address this, we mapped genetic variants that are associated with eQTLs, ribosome occupancy (rQTLs), or protein abundance (pQTLs). We found that most QTLs are associated with transcript expression levels, with consequent effects on ribosome and protein levels. However, eQTLs tend to have significantly reduced effect sizes on protein levels, which suggests that their potential impact on downstream phenotypes is often attenuated or buffered. Additionally, we identified a class of cis QTLs that affect protein abundance with little or no effect on messenger RNA or ribosome levels, which suggests that they may arise from differences in posttranslational regulation.

To understand the links between genetic and phenotypic variation, it may be essential to first understand how genetic variation impacts the regulation of gene expression. Previous studies have evaluated the association between variation and transcript expression in humans (*1–3*). Yet protein abundances are more direct determinants of cellular functions (*4*), and the impact of genetic differences on the multistage process of gene expression through transcription and translation to steady-state protein levels has not been fully characterized. Studies in model organisms have shown that variations in mRNA and protein expression levels are often uncorrelated (*5–8*). Comparative studies (*9–13*) have suggested that protein expression evolves under greater evolutionary constraint than transcript levels (*14*) and have provided evidence consistent with buffering of protein expression with respect to variation introduced at the transcript level. Yet, in contrast to comparative work, there are few reports of quantitative trait loci (QTLs) associated with protein levels (pQTLs) in humans (*15–17*).

Here, we present a unified analysis of the association of genetic variation with transcript

Refining deep brain stimulation to emulate optogenetic treatment of synaptic pathology

Meaghan Creed *et al.*

Science **347**, 659 (2015);
DOI: 10.1126/science.1260776